

## **Design and Study of a Packed Absorption Column for CO<sub>2</sub> Scrubbing**

### **Dr. Maddalena Fanelli, Michigan State University**

Dr. Maddalena Fanelli is a Teaching Specialist in the Department of Chemical Engineering and Materials Science at Michigan State University. Dr. Fanelli teaches and coordinates a number of undergraduate courses and laboratories, helping students learn chemical engineering fundamentals and gain hands-on experience.

### **Alexis Chuong**

### **Mr. Robert Selden, Michigan State University**

Mr. Robert Selden is a Research and Instructional Equipment Technologist in the Department of Chemical Engineering & Material Science at Michigan State University. He provides technical and maintenance support for both Teaching and Research Laboratories.

# **Design and Study of a Packed Absorption Column for CO<sub>2</sub> Scrubbing**

## **Abstract**

Absorption is one of the most widely used industrial methods for purification of high-volume gas streams. Therefore, the availability of absorption equipment in a teaching lab can help chemical engineering students better understand both the fundamentals and practical applicability of mass transfer principles. A small-scale absorption column was designed and built for our unit operations teaching lab to absorb carbon dioxide from an air stream with a dilute sodium hydroxide solution. The packing support, liquid outlet valve, and liquid flow distributor were selected and tested to promote smooth flow and good distribution. The flooding and absorption performance of the column were found to be in good agreement with literature. Guidelines for the construction of this column can help others build similar equipment for their teaching or research labs.

## **Introduction**

Absorption is one of the most widely used industrial methods for purification of high-volume gas streams. A two-floor absorption column in Michigan State University's Chemical Engineering Unit Operations teaching lab is regularly used to absorb carbon dioxide from an air stream with a dilute sodium hydroxide solution. The existing system includes a 150 gal liquid feed tank, a centrifugal pump, a set of valves and a flowmeter to regulate the flow of liquid to the column, and a 144" tall, glass column connected to a liquid overflow drum. The gas feed stream is a mixture of compressed air, from the building supply line, and carbon dioxide (CO<sub>2</sub>), from a compressed cylinder. Both gas streams are metered through mass flow controllers. The vapor exit stream is sampled with a Siemens infrared (IR) sensor capable of measuring CO<sub>2</sub> concentrations up to 10 vol%.

With appropriate guidance and careful attention to safe practices, operation of the existing glass absorption column is relatively straight forward. However, the two-floor stand is not mobile and its operation requires careful attention and monitoring by three-member student groups. Two-person teams find it difficult to master, as they have to simultaneously check for flooding, monitor flows and concentrations, and adjust the liquid drainage valve to maintain sealing and prevent escape of vapor through the bottom exit stream. In addition, the packing within the column is essentially fixed, since a change would require disassembly of the multi-floor glass column.

To expand access of the equipment to smaller student teams, to provide a direct comparison between equipment of different scales, and to allow easy testing of different packing materials, we designed a small-scale absorption column, connecting liquid and vapor inlets and sampling lines to those of the existing system.

The current paper focuses on detailing the components used to construct the small column, providing a small set of flooding and absorption results that confirm its performance. A list of parts and some representative figures are included in the appendix. Although the data presented in this paper are limited, we are confident that they reflect the viability of the system. In the spring semester of 2023, the column was used in the teaching lab and the data set was expanded for better validation.

## The Absorption Column

The existing large-scale packed column is made of glass, spans two floors, and has an ID of 3" and a packing height of 100". The main body of the small-scale column consists of a 2" Schedule 40, transparent PVC pipe, with an ID of 2" and a packing height of approximately 16.5". Both columns are packed with 6 mm ceramic Intalox saddles. A simplified schematic of the small-scale column is shown in Figure 1.

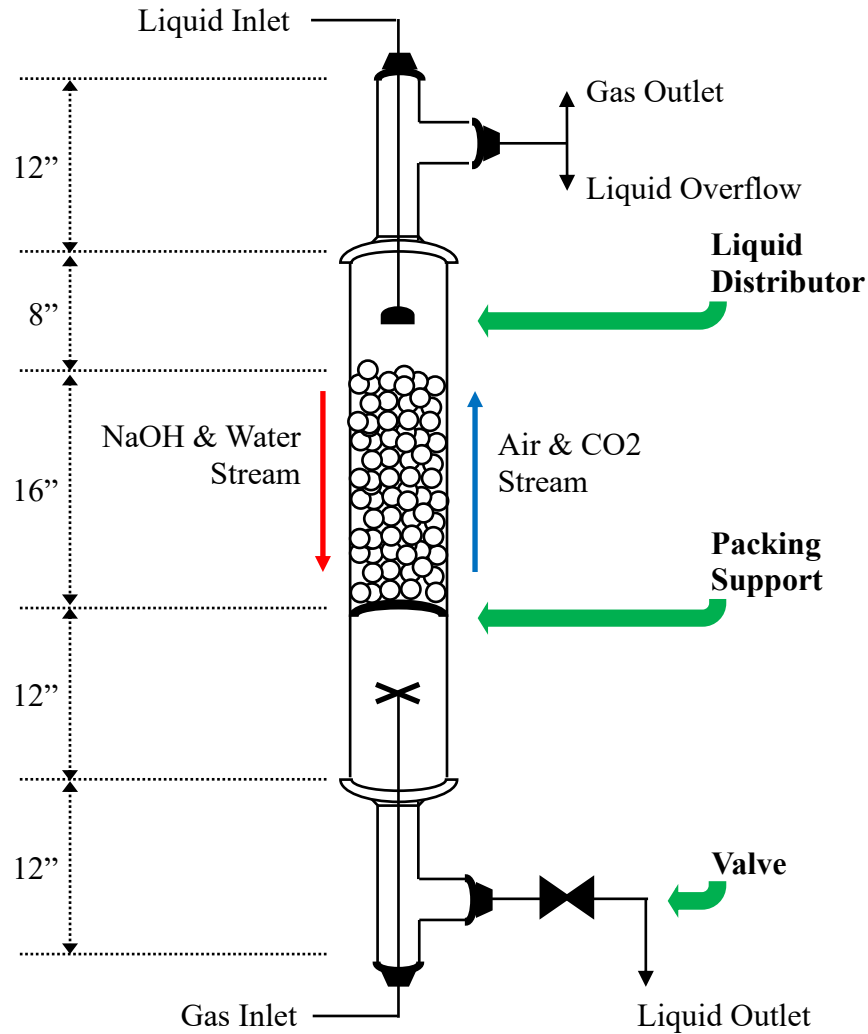


Figure 1. Simplified schematic of the small-scale packed absorption column. Although approximate heights are noted, proportions are not to scale (i.e., the internal diameter of the column is 2"). Components that require particular attention are identified with bold lettering.

Construction of the column involves selection and technically expert assembly of appropriate fittings and parts, as detailed in the appendix. Proper selection of three components is particularly critical to the operation of the column [1].

- The liquid distributor needs to provide an evenly distributed flow of liquid over the cross section of the column. This allows maximum interaction between the gas and liquid streams. Several distributors were connected to a sink faucet and tested. The standard aerators shown in Figures 2a and b achieved even distributions only at high flow rates, associated with column flooding. The nozzle shown in Figure 2c led to uniform spraying at low flow rates but was set aside because of chemical compatibility concerns. The cross-pipe shown in Figure 2d was suitable for the current trials, leading to an adequately uniform flow profile.

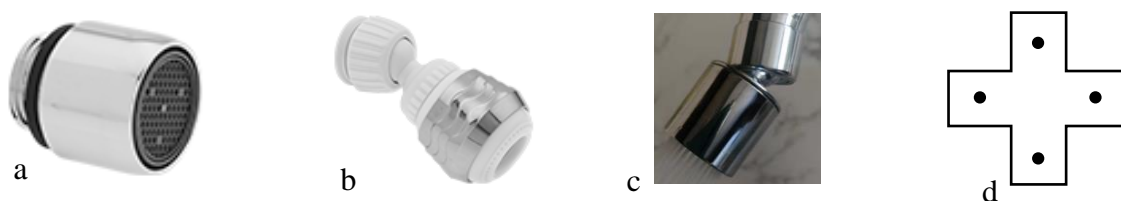


Figure 2. Liquid distributors evaluated: a) & b) McMaster Carr faucet aerators, Catalog No. 2675K34 and 2755K13, respectively; c) Boarne faucet nozzle aerator; d) cross-pipe with 1/16" diameter holes drilled 0.5" from the center.

- The packing support needs to sustain the packing while allowing the continuous passage of both gas and liquid through the column [2]. A fine disc, made from a 20 x 20 (20 holes per in<sup>2</sup>, in both directions) stainless steel mesh, was initially used as the support, since it was readily available in the desired diameter. However, it led to discontinuous, interrupted flow through the column. High capillary pressure caused slug flow behavior, as gas and liquid competed for the mesh openings. The support was changed to a 6 x 6 mesh, as the larger openings lead to lower capillary pressure and continuous, smooth flow of both phases. Figure 3 shows the relative pore size of the meshes.

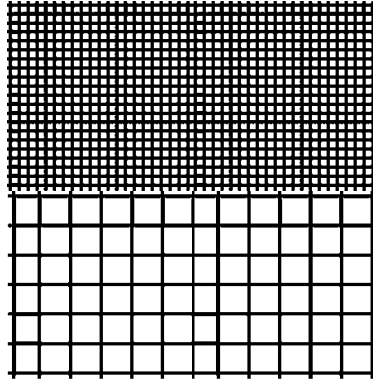


Figure 3. Representative sketch of the tested packing supports purchased from McMaster-Carr. Top: 20 x 20 (20 holes per in<sup>2</sup>, in both directions) stainless steel mesh; bottom: 6 x 6 stainless steel mesh.

- The liquid discharge valve needs to be easily adjustable, preventing gas from escaping through the bottom of the column while allowing fine control of the liquid flow. Figure 4 shows four valves evaluated for this application.



Figure 4. Tested valves, numbered accordingly: (#1) John Guest, 3/8" OD ball valve, (#2) SMC, 1/2" OD needle valve, (#3) Flow-Rite Controls, 1/2" OD needle pinch valve, (#4) Asahi/America 1/2" PVC globe valve (Item #1261005).

Evaluation of the valves involved estimating their capacity factor,  $C_V$  (in GPM/√psi), to determine whether they allow control of flow within the desired operating range. Valve 3 was inserted over a 3" long 1/4" ID, 3/8" OD tube. For Valves 1 through 3, the small column was run with air and water. With each valve fully open, the air flow rate was set to 10 LPM (the envisioned minimum for our experiments) and the flow rate of the liquid through the column was varied to identify the maximum liquid flow rate that would allow steady state operation (a constant liquid level in the region below the gas inlet port). While running this experiment, the tubing between the column and the valve was also checked to ensure that no air escaped through the liquid port.

The liquid flow rate and the pressure upstream of the valve were measured and used to determine an effective valve capacity factor, adopting Equation 1,

$$q = C_V \sqrt{\Delta p_{valve}} \quad (1)$$

where  $q$  is the volumetric flow rate of water (in GPM), and  $\Delta p_{valve}$  is the pressure drop across the valve (in psi). The highest capacity factor among the three valves was 1.8 GPM/ $\sqrt{\text{psi}}$  for Valve 3, corresponding to a maximum flow rate of 1.4 LPM. Valve 4 was evaluated separately, flowing water at 1.4 LPM through the fully open valve and determining the corresponding pressure drop. Figure 5 shows the resulting effective capacity factor for each valve. Given its higher capacity (averaging 2.1 GPM/ $\sqrt{\text{psi}}$ ), better handling, and more easily controlled performance, Valve 4 was selected for the stand.

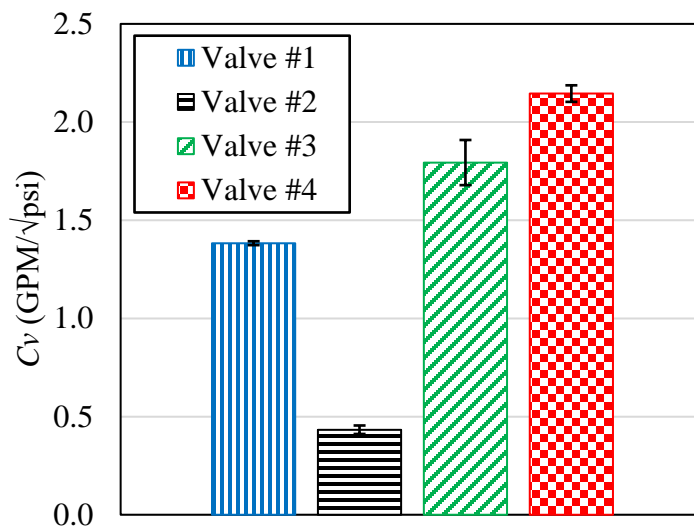


Figure 5. Average effective  $C_v$  for each valve tested with standard deviation as error bars. Two replicates were performed for Valves 1, 2, and 3; three replicates for Valve 4.

It is important to note that the lower section of the column needs to be sufficiently sized to accommodate changes in the liquid level that arise in response to changes in the liquid flow rate. The use of transparent material for this section of the column makes it possible to see the liquid level and verify when the system is at steady state.

### **Infrared (IR) Meter Calibration**

Gauging absorption performance hinges on the accurate measurement of the carbon dioxide concentration in the inlet and outlet vapor streams of the column. Hence, a test was run to verify that the IR meter measures  $\text{CO}_2$  concentration accurately, that there are no leaks in the system, and that inlet and outlet  $\text{CO}_2$  concentration measurements are consistent.

The column was run with water, air, and  $\text{CO}_2$ . The  $\text{CO}_2$  concentration was changed using the mass flow controllers (MFC's) placed on the air and  $\text{CO}_2$  supply lines. The set rates shown on the MFC's, and the IR meter reading were recorded and used to generate the calibration curve shown in Figure 6. The consistency between the inlet and outlet measurements demonstrated that there was no change in the  $\text{CO}_2$  concentration because of leaks or absorption in the water stream. The accuracy of the IR meter was also supported by the diagonal alignment of the calculated and measured  $\text{CO}_2$  concentrations.

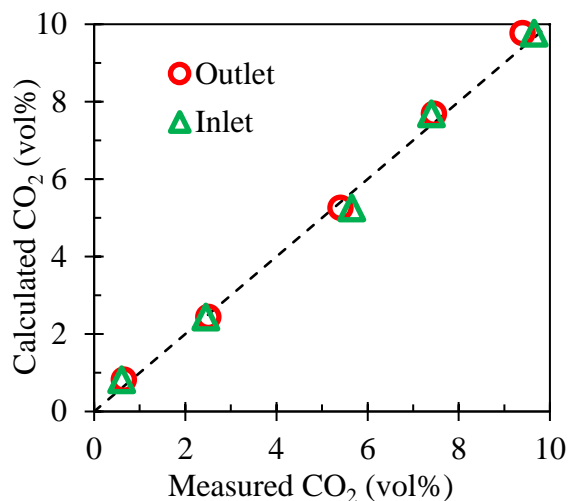


Figure 6. Comparison of calculated and measured inlet and outlet CO<sub>2</sub> concentrations in the gas stream. The measured values were read directly from the IR meter, while the calculated values were determined using the flow rate values shown on the MFC's.

### **Flooding Studies**

The maximum flows of gas and liquid through the column dictate the operating window for the system. Hence, before running absorption tests, flooding studies were performed to determine the operating limits of the column and estimate the packing factor,  $F_p$ . The column was run with air and water and the liquid flow rate was slowly increased at set gas flow rates until flooding occurred. As the results reported in Figure 7 indicate, the flooding data superimposed on the Generalized Pressure Drop Chart [3] lead to an estimate of  $800 \text{ ft}^{-1}$  for the packing factor, within 10% of published values (according to Saint-Gobain,  $725 \text{ ft}^{-1}$  for 6 mm Proware Saddles made to the original Intalox specifications [4]). The measured flow rates used to obtain the flooding estimates are noted in Table 1.



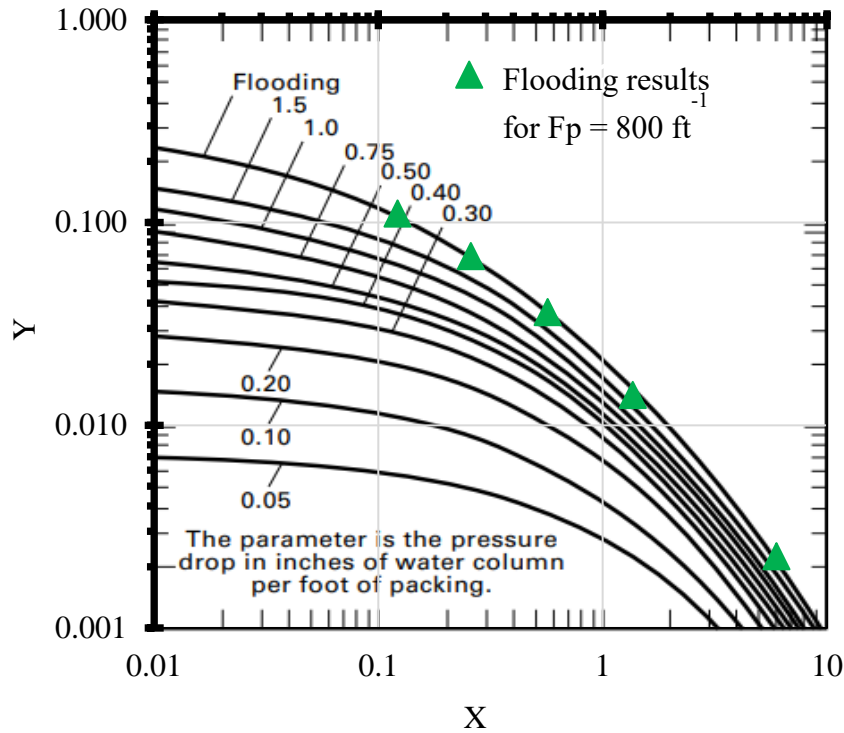


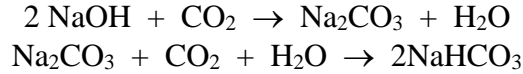
Figure 7. Overlay of flooding data onto the Generalized Pressure Drop Chart to estimate the packing factor,  $F_P$  [3]. Water and air are the working fluids. The axes values are  $Y = \frac{u_V^2 F_P}{g} \left( \frac{\rho_V}{\rho_L} \right)$  and  $X = \frac{L M_L}{V M_V} \left( \frac{\rho_V}{\rho_L} \right)$ , where  $u_V$  is the superficial gas velocity,  $g$  is gravitational acceleration,  $\rho_L$  and  $\rho_V$  are the liquid and vapor densities, respectively,  $L$  and  $V$  are the liquid and molar flow rates, respectively, and  $M_L$  and  $M_V$  are the molecular weight of the liquid and vapor, respectively.

Table 1. Gas and liquid flow rates used to obtain the flooding data reported in Figure 7. Experiments were run at ambient conditions, 25 °C, 1 atm.

| gas flow rate<br>(LPM) | liquid flow rate<br>(LPM) |
|------------------------|---------------------------|
| 10                     | 2.1                       |
| 25                     | 1.2                       |
| 40                     | 0.8                       |
| 55                     | 0.5                       |
| 70                     | 0.3                       |

## Absorption Results

The reactive absorption of CO<sub>2</sub> with sodium hydroxide (NaOH) was used to determine the overall volumetric, gas-based mass transfer coefficient ( $K_y a$ ) and gauge the performance of the column at different flow rates. The liquid-phase reactions that take place when the CO<sub>2</sub> is absorbed into the liquid are given below:



The system is run such that there is a stoichiometric excess of NaOH in the liquid to fully react with the absorbed species and maintain an equilibrium CO<sub>2</sub> concentration of zero at the liquid interface.  $K_y a$  is determined as a function of gas and liquid flow rates by measuring the concentration of CO<sub>2</sub> in the inlet and outlet gas streams.

In the current experiments, an aqueous 0.1 M NaOH solution and an air stream containing 9 vol% CO<sub>2</sub> were fed to the column. Equation 2 is used to determine the overall, gas-based number of transfer units,  $N_{OG}$ , using the mole fraction of CO<sub>2</sub> in the inlet and outlet gas stream,  $y_{in}$  and  $y_{out}$ , respectively. The CO<sub>2</sub> concentration in equilibrium with the liquid at the interface,  $y^*$ , is assumed to be zero. The overall, gas-based height of a transfer unit,  $H_{OG}$ , is calculated from the total height of the packed column,  $l_T$ , using Equation 3. The mass transfer coefficient is calculated from Equation 4, knowing the cross-sectional area of the column,  $S$ , and the molar flow rate of the gas,  $V$  [3].

$$N_{OG} = \int_{y_{out}}^{y_{in}} \frac{dy}{y - y^*} \quad (2)$$

$$l_T = H_{OG} N_{OG} \quad (3)$$

$$H_{OG} = \frac{V}{K_y a \cdot S} \quad (4)$$

The results of preliminary absorption trials are reported in Figure 8. The mass transfer coefficient is reported as a function of liquid load (volumetric flux) for two different gas flow rates. For perspective on the quality of the results, the graph includes data extracted from Koch-Glitsch's technical brochure on plastic packing and column internals, pertaining to their Super Intalox Saddles #3 [5]. Although details of the size of their packing are not clear, the consistency of the trend and the magnitude are evident. The data collected and used to perform the analysis are presented in Table 2. For our system, the results indicate that increased liquid flow increases mass transfer, while gas flow had no apparent effect on performance.

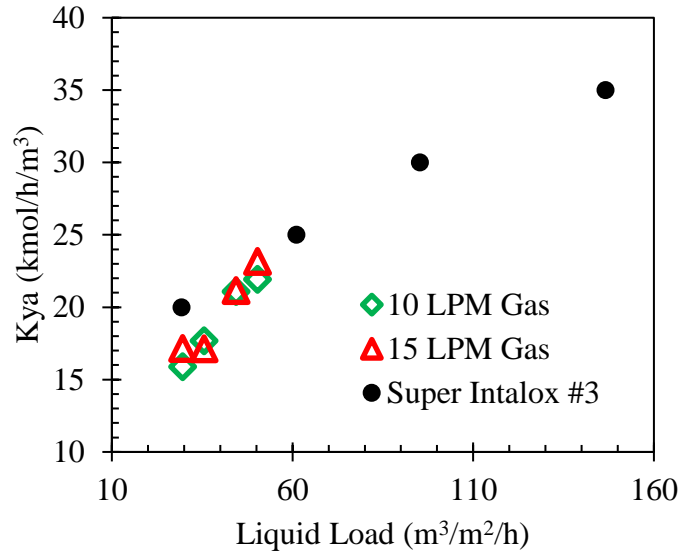


Figure 8. Preliminary mass transfer results for varying liquid and gas flow rates. Data extracted from Koch-Glitsch's technical brochure on their plastic Super Intalox Saddles #3 are included for reference [5].

Table 2. Absorption data used to construct Figure 8. Standard deviation is included as uncertainty for the inlet concentration.

| liquid flow rate (LPM) | gas flow rate (LPM) | inlet CO <sub>2</sub> concentration (vol%) | outlet CO <sub>2</sub> concentration (vol%) |
|------------------------|---------------------|--|---|
| 1.0                    |                     |  | 5.500                                       |
| 1.2                    | 10                  | 9.050±0.283                                | 5.200                                       |
| 1.5                    |                     |  | 4.675                                       |
| 1.7                    |                     |  | 4.525                                       |
| 1.0                    |                     |  | 6.550                                       |
| 1.2                    | 14.5                | 9.325±0.247                                | 6.375                                       |
| 1.5                    |                     |  | 5.950                                       |
| 1.7                    |                     |  | 5.650                                       |

## **Conclusions**

A small-scale absorption column was constructed and tested to validate its performance. Flooding and absorption results closely aligned with expected trends. Both the original and new absorption columns were used in our teaching lab in the spring semester of 2023. Students successfully performed flooding studies on both systems, comparing results to ascertain consistency. To reduce caustic consumption, absorption experiments were performed on the new, smaller column alone. Students reported appreciation for dealing with both the large and small scale equipment, seeing what happens within the column, at eye level, and confirming the adherence of experimental results with textbook predictions and published trends. We hope that this work may serve as a guide to others wanting to implement small-scale absorption studies in their laboratories.

## **Acknowledgements**

This work was made possible by the Chemical Engineering and Materials Science Department, at Michigan State University.

## **References**

- [1] G. Towler and R. Sinnott, *Chemical Engineering Design - Principles, Practice and Economics of Plant and Process Design*, 3<sup>rd</sup> Ed., Butterworth-Heinemann, pp. 693-717, 2021.
- [2] W. A. Gaakeer, M. H. J. M. de Croon, J. van der Schaaf and J. C. Schouten, "Liquid-liquid slug flow separation in a slit shaped micro device," *Chemical Engineering Journal*, Vol. 207-208, pp. 440-444, 2012.
- [3] J. D. Seader, E. J. Henley and K. K. Roper, *Separation Process Principles*, 3<sup>rd</sup> Ed., John Wiley & Sons, Inc., p. 236-244, 2011.
- [4] Saint-Gobain, *Proware<sup>TM</sup> Ceramic Mass Transfer Packings*, <https://www.norpro.saint-gobain.com/products/mass-transfer-products/proware-ceramic-mass-transfer-packings>, 2022.
- [5] Koch-Glitsch, *Plastic packing and Column Internals*, <https://koch-glitsch.com/technical-documents/brochures/plastic-packing-and-column-internals>, Bulletin KGPPCI-1.1, Rev. 05-2019.

## Appendix

Table. A1. List of parts used to construct the small-scale absorption column. Part IDs refer to Figures A1 and A2. Prices are subject to change. Some smaller tubing and components, pertaining to the inlet and outlet ports, are not included, as they can be more easily selected. The table also excludes PVC cement, used to attach the parts. Additional valves that could provide fine metering of the liquid flow include Plastomatic's Series ZC ½" PVC manual Control Ball Valve, with 15degree V-ball, threaded connectors and EPDM seals (Model Number MBV050EPT-PV-C1), and Chemline Plastics's SM Series 1" PVC manual Metering Ball Valve, with threaded connectors and EPDM O-rings (Model Number SM2-A-010-E-T).

| Part ID | Part Description  | McMaster-Carr Part # | Quantity | Part Price (\$) | Full Price (\$) |
|---------|---|----------------------|----------|-----------------|-----------------|
| 1       | 3/8" x 3/8" Push to Connect Fitting                                 | 1901K32              | 3        | 10.70           | 32.10           |
| 2       | 3/8" Stainless Steel Tube, cut into two                             | 8989K76              | 3'       | -               | 12.88           |
| 3       | 3/8" x 3/8" Compression Fitting                                     | 50775K335            | 2        | 2.33            | 4.66            |
| 4       | 1" PVC Tee, Clear   | 9161K33              | 2        | 35.18           | 70.36           |
| 5       | 2" to 1" Reducing Coupling  | 4881K744             | 2        | 21.65           | 43.30           |
| 6       | 2" PVC Flanges  | 6826K176             | 4        | 19.95           | 79.80           |
| 7       | 6 x 6 Stainless Steel Wire Cloth                                    | 85385T35             | 1        | 18.46           | 18.46           |
| 8       | 2" PVC Coupling, Clear  | 9161K46              | 2        | 45.78           | 91.56           |
| 9       | 1/4" Stainless Steel Cross  | 446K312              | 2        | 17.79           | 35.58           |
| 10      | 2" PVC Pipe, Clear  | 49035K28             | 4'       | -               | 51.19           |
| 11      | 1/2" Threaded Asahi/America PVC Globe Valve (1261005 Asahi/America) | 47535K21             | 1        | 61.62           | 61.62           |
| 12      | 5/8"-11 Chemical Resistant Nuts                                     | 94806A044            | 16       | 3.78            | 60.48           |
| 13      | 5/8"-11 Nylon Threaded Rod, 1' cut into eight                       | 98831A110            | 3        | 16.49           | 49.47           |
| 14      | 1/4" Stainless Steel Plug   | 446K562              | 8        | 1.05            | 8.40            |
| 15      | 2" Viton Gaskets  | 9473K616             | 2        | 5.22            | 10.44           |
| 16      | 1" to 3/8" Threaded PVC Reducing Bushing                            | 4596K413             | 3        | 6.68            | 20.04           |
| 17      | 1" Threaded Adapter   | 9161K53              | 4        | 21.45           | 85.80           |
| TOTAL   |   |                      |          |                 | 736.14          |

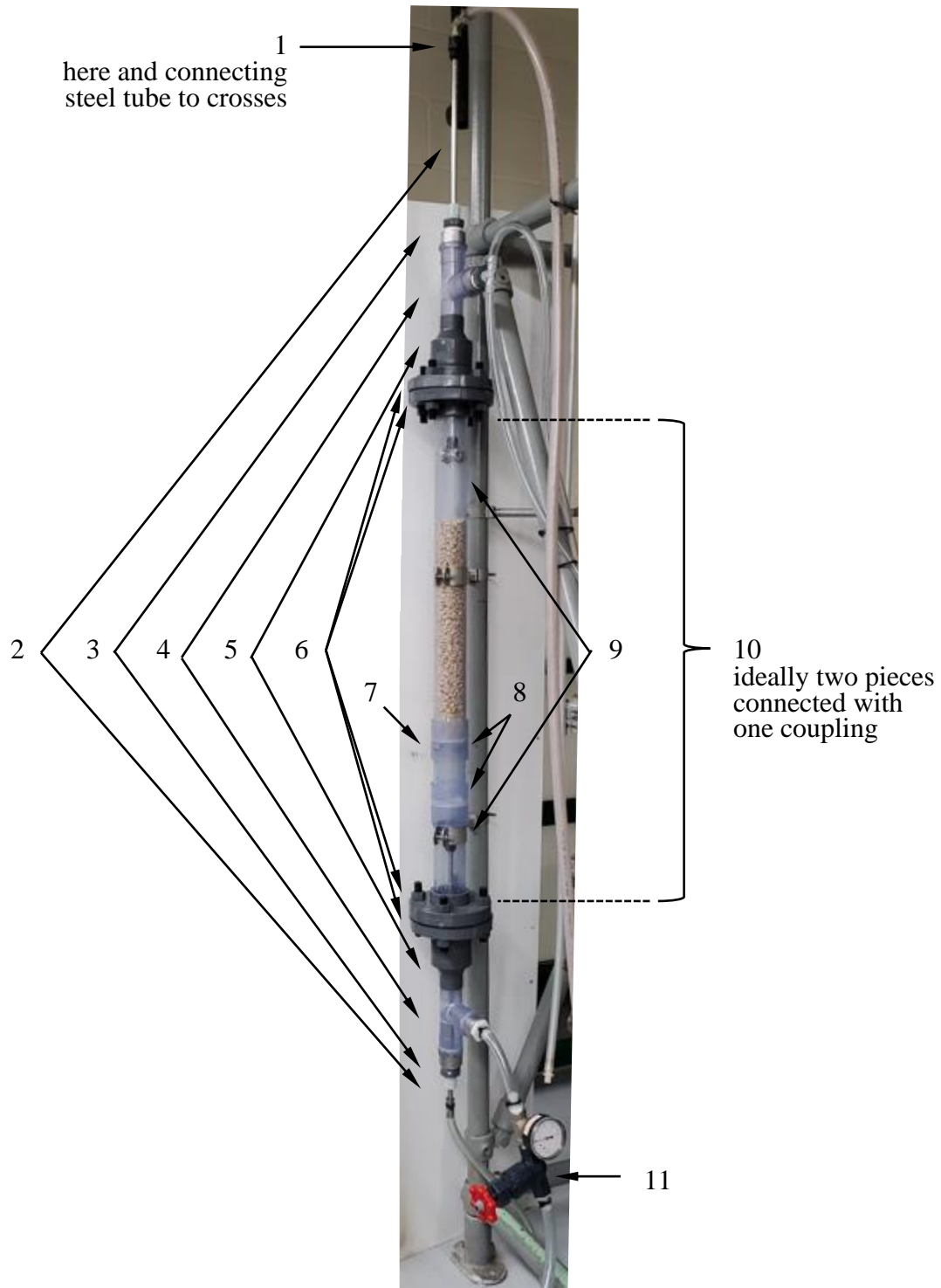


Figure A1. Small absorption column with main component parts identified and described in Table A1.

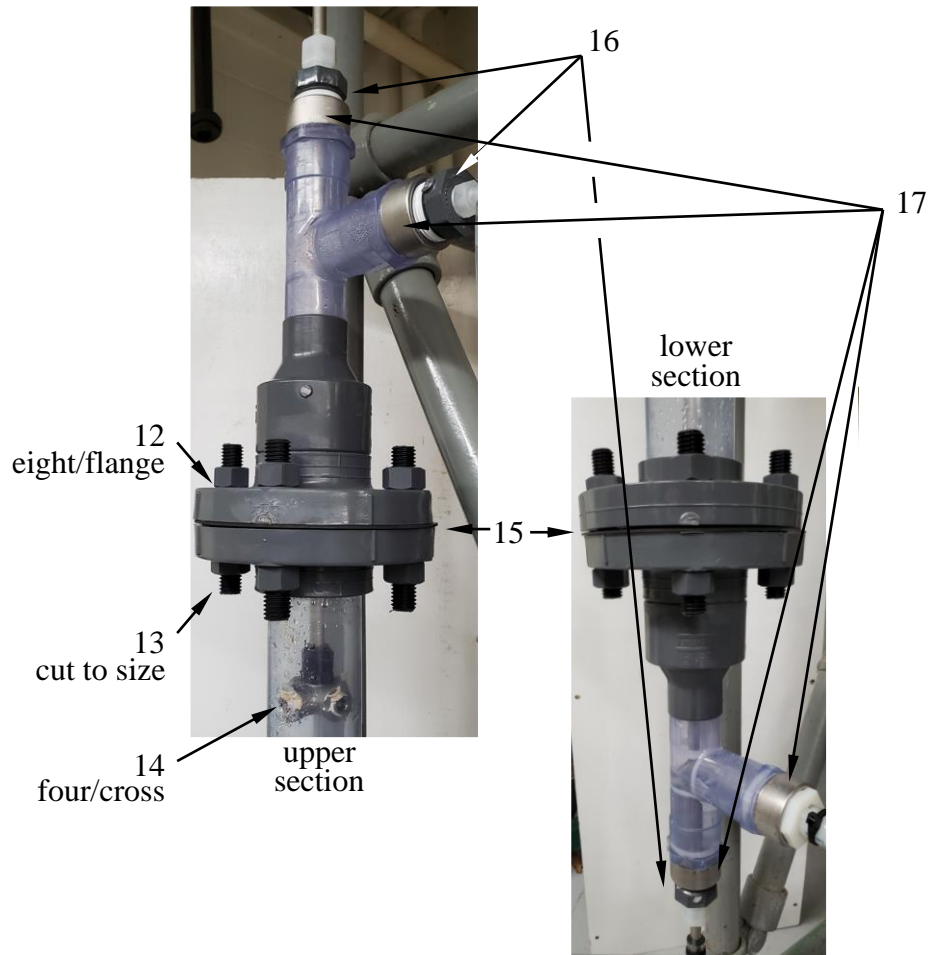


Figure A2. Upper and lower sections of the small absorption column. Identified parts are described in Table A1.